

Supporting Information

Nodulisporic acid E biosynthesis: *In vivo* characterisation of NodD1, an indole-diterpene prenyltransferase that acts on an emindole SB derived indole-diterpene scaffold

Kyle C. Van de Bittner,^{a†} Rosannah C. Cameron,^{a†} Leyla Y. Bustamante,^{a†} Rudranuj Bundela,^a Sarah A Kessans,^b Jan Vorster,^c Matthew J. Nicholson,^{*a} Emily J. Parker^{*a,d}

^a. Ferrier Research Institute, Victoria University of Wellington, Kelburn, Wellington 6012, New Zealand.

^b. Biomolecular Interaction Centre and School of Biological Sciences, University of Canterbury, PO Box 4800, Christchurch 8140, New Zealand.

^c. School of Chemical and Physical Sciences, Victoria University of Wellington, PO Box 6012, Wellington, New Zealand.

^d. Maurice Wilkins Centre for Molecular Biodiscovery, New Zealand.

† These authors contributed equally to this work

Table of Supplementary Tables

Table S1. Similarity matrix for fungal aromatic prenyl transferases based on ClustalW alignment of amino acid sequences.....	6
Table S2. ¹ H and ¹³ C NMR assignment of nodulisporic acid E (NAE) 1 in CDCl ₃ . Spectra depicted in Figures S7 to S11 and raw spectra data can be found in the corresponding FID files.....	7
Table S3. Database accession numbers for amino acid sequences of enzymes investigated in this study.....	8
Table S4. Table of fungal species used in this study.	9
Table S5. Table of fungal strains generated in this study.	9
Table S6. Multistep acetonitrile gradient used for LCMS analysis of fungal extracts.....	10
Table S7. PCR primers for amplification of transcription unit modules (TUMs).	11
Table S8. Synthetic gene sequence for nourseothricin resistance gene (<i>natR</i>).	12
Table S9. MIDAS Level-1 plasmid library: Assembly of TUMs in pML1.....	13
Table S10. MIDAS Level-2 plasmid library: Assembly of TUs in pML2 destination vectors.	13
Table S11. MIDAS Level-3 plasmid library: Multigene assemblies in pML3.....	14

Table of Supplementary Figures

Figure S1. Secondary-metabolic steps in the biosynthetic pathway of IDTs that give rise to the diverse IDT structures. Arrows represent enzymatic steps in IDT biosynthesis and the enzyme color corresponds to the number of the specific step in the pathway. The biosynthetic pathways for paspaline-derived IDTs, for which all previously characterized IDT PTs belong to, is highlighted with the red box.	15
Figure S2. Depiction of AtmD substrate promiscuity tested by Liu et al 2013 ¹⁹ using <i>in vitro</i> feeding experiments. Theoretical minor products are indicated by an asterisk (*).	16
Figure S3. Extracted ion chromatograms (EICs) used to detect paxilline 3 (11.3 minutes, [M+H] ⁺ 436.3 m/z) and NAF 2 (12.6 minutes, [M+H] ⁺ 436.3 m/z). The 130.3 m/z EIC is used to confirm the presence of a nonprenylated IDT. Fragmentation energies of 100 V and 200 V were used to capture the 436.3 m/z and 130.3 m/z EICs, respectively. All 436.3 m/z and 130.3 m/z EICs have been scaled to 1,100,000 AU and 600,000 AU, respectively.	17
Figure S4. Extracted ion chromatograms (EICs) used to detect monoprenylated products. The 504.3 m/z EICs correspond to paxilline 3 or NAF 2 that contain a single prenyl group, the 502.3 m/z EICs correspond to an oxidized form (i.e. -2H) of the monoprenylated products, and the 198.3 m/z EICs correspond to the major ion fragment of monoprenylated paxilline or NAF. Fragmentation energies of 100 V was used to capture the 504.3 m/z and 502.3 m/z EICs, and a fragmentation energy of 200 V was used to capture the 198.3 m/z EICs. All 504.2 m/z, 502.4 m/z and 198.3 m/z EICs have been scaled to 700,000 AU, 140,000 AU, and 200,000 AU, respectively. Novel monoprenylated compounds, not present in parental strains, are indicated by an asterisks (*).	18
Figure S5. Extracted ion chromatograms (EICs) used to detect bisprenylated products. The 572.4 m/z EICs correspond to paxilline 3 or NAF 2 that contain a two prenyl groups, the 570.4 m/z EICs correspond to an oxidized form (i.e. -2H) of the bisprenylated products, and the 266.4 m/z EICs correspond to the major ion fragment of bisprenylated paxilline or NAF. Fragmentation energies of 100 V was used to capture the 572.4 m/z and 570.4 m/z EICs, and a fragmentation energy of 200 V was used to capture the 266.4 m/z EICs. All 572.4 m/z, 570.4 m/z and 266.4 m/z EICs have been scaled to 1,400,000 AU, 350,000 AU, and 350,000 AU, respectively. Novel bisprenylated compounds, not present in parental strains, are indicated by an asterisks (*).	19
Figure S6. High-Resolution Mass Spectrometry (HRMS) results for NAE 1 characterization. A depicts the HRMS of NAE 1 with a fragmentation energy of 200 V showing the [M+H] ⁺ parent ion at 572.4101 m/z and B shows the HRMS of NAE 1 with a fragmentation energy of 300 V showing the fragmentation of the [M+H] ⁺ parent ion at 572.4080 m/z to the key bisprenylated IDT [M+H] ⁺ ion of 266.1893 m/z.	20
Figure S7. ¹ H-NMR spectra for NAE 1 standard in CDCl ₃ at 600 MHz.	21
Figure S8. ¹³ C-NMR spectra for NAE 1 standard in CDCl ₃ at 150 MHz.	22
Figure S9. HMBC-NMR spectra for NAE 1 standard in CDCl ₃ at 600 MHz.	23

Figure S10. COSY-NMR spectra for NAE 1 standard in CDCl ₃ at 600 MHz.	24
Figure S11. HMQC-NMR spectra for NAE 1 standard in CDCl ₃ at 600 MHz.	25
Figure S12. TLC of ten HPF1:pRC63 (<i>nodD1</i>) transformant extracts. Lanes: S = NAF 2, 0 = HPF1 + pRC13 (non-NAE producing strain), 1-10 = HPF1:pRC63 (<i>nodD1</i>) transformants. NAF 2 is identified by a green spot on the TLC plate and NAE 1 is identified by a yellow spot on the TLC plate. This TLC indicates that NAE 1 is present in at least nine of ten transformants (lanes 2 to 10).	26
Figure S13. TLC of ten HPF1:pRC18 (<i>janD</i>) transformant extracts. Lanes: S = NAF 2, 1-10 = HPF1:pRC18 (<i>janD</i>) transformants. NAF 2 is identified by a green spot on the TLC plate. No new prenylated IDTs were detected in any of the ten transformant extracts by TLC or LC-MS analysis.	27
Figure S14. TLC of HPF1:pRC64 (<i>atmD</i>) transformant extracts. Lanes: S = NAF 2, 1-10 = HPF1:pRC64 (<i>atmD</i>) transformants. NAF 2 is identified by a green spot on the TLC plate. No new prenylated IDTs were detected in any of the ten transformant extracts by TLC or LC-MS analysis.	28
Figure S15. TLC of six PN2013:pRC63 (<i>nodD1</i>) transformant extracts. Lanes: S = paxilline 3, 0 = PN2013 (wildtype <i>P. paxilli</i> that does not produce detectable prenylated products), 1-6 = PN2013:pRC63 (<i>nodD1</i>) transformants. Paxilline 3 is identified by a green spot on the TLC plate and prenylated paxillines are identified by a yellow spot on the TLC plate. This TLC indicates that prenylated paxillines are present in at least two of six transformants (lanes 3 and 4).	29
Figure S16. TLC of five PN2013:pRC18 (<i>janD</i>) transformant extracts. Lanes: 0 = PN2013 (wildtype <i>P. paxilli</i> that does not produce detectable prenylated products), 1-5 = PN2013:pRC18 (<i>janD</i>) transformants. Paxilline 3 is identified by a green spot on the TLC plate and prenylated paxillines are identified by a yellow spot on the TLC plate. This TLC indicates that prenylated paxillines are present in at least three of five transformants (lanes 1, 3 and 5).	30
Figure S17. TLC of ten PN2013:pRC64 (<i>atmD</i>) transformant extracts. Lanes: S = paxilline 3, 0 = PN2013 (wildtype <i>P. paxilli</i> that does not produce detectable prenylated products), 1-10 = PN2013:pRC64 (<i>atmD</i>) transformants. Paxilline 3 is identified by a green spot on the TLC plate and monoprenylated paxillines are identified by a blue spot on the TLC plate. This TLC indicates that monoprenylated paxillines are present in at least seven of ten transformants (lanes 1, 2, 3, 5, 6, 8 and 9).	31

Supplementary Materials and Methods

The following protocols were completed as described in Van de Bittner et al 2018¹

gDNA isolation transcription unit module (TUM) amplification

Preparation of similarity matrices and phylogenetic trees for cluster identification

The following protocols were completed as described in van Dolleweerd et al 2018²

Molecular biology.
Bacterial and fungal strains.
Construction of DNA constructs using the MIDAS cloning system.
Protocols for MIDAS Level-1 module cloning.
Protocols for MIDAS Level-2 TU assembly.
Protocols for MIDAS Level-3 multigene assembly.
Media and reagents used for fungal work.
Fungal Protocols – Protoplast Preparation.
Fungal Protocols – Transformation of *P. paxilli*.
Indole diterpene production and extraction.
Normal phase thin-layer chromatography (TLC).
Reverse phase liquid chromatography-mass spectrometry (LC-MS).
Large scale indole diterpene purification for NMR analysis.

Indole-diterpene production and extraction

Fungi, listed in Tables S4 (parent strains) and S5 (transformed strains) were analysed for production of indole diterpenes. Ten independent colonies were analysed from each transformation unless only a smaller number of transformants were available (six for PN2013:pRC63, and five for PN2013:pRC18). Fungi were grown in 25 mL of CDYE medium with trace elements in 125 mL Erlenmeyer flasks capped with cotton wool for 7 days at 28°C in shaker cultures (≥200 rpm). Mycelia were isolated from fermentation broths by filtration through nappy liners, transferred to 2 mL screw-cap tubes containing 500 mL ethyl acetate and 0.1 g of 1.6 mm stainless steel beads (Next Advance). Mycelia were homogenized at 6 m/s for 40 sec. using a FastPrep-24 5G homogenizer equipped with a QuickPrep adapter. Tubes were centrifuged for 10 min at 17,000 xg and the top organic layer was used for downstream TLC and LCMS analysis.

Normal phase TLC

The ethyl acetate supernatant (containing extracted indole-diterpenes) was used for TLC analysis on solid phase silica gel on aluminium foils (Merck). Indole-diterpenes were chromatographed with 9:1 or 19:1 chloroform:methanol and visualised with Ehrlich's reagent (1% (w/v) *p*-dimethylaminobenzaldehyde in 24% (v/v) HCl and 50% ethanol).

Reverse phase LCMS

Samples were prepared for LCMS from selected transformants that were identified by TLC. Accordingly, the ethyl acetate supernatant (containing extracted indole-diterpenes) was transferred to a 2 mL glass vial and the solvent was evaporated overnight. Contents were resuspended in 100% acetonitrile and filtered through a 0.2 µm membrane into a LCMS vial. LCMS samples were chromatographed on a reverse phase Thermo Scientific Accucore 2.6 µm C18 (50 × 2.1 mm) column attached to an Agilent 1260 Infinity II LC system run at a flow rate of 0.300 mL/minute and eluted with aqueous solutions of acetonitrile containing 0.01% formic acid using a multistep gradient method (Table S6). Mass spectra were captured through in-line analysis on an InfinityLab 6100 series LC/MSD single quadrupole mass spectrometer (Agilent). High-resolution mass spectra were captured using direct injection onto an Agilent 6530 quadrupole-time-of-flight mass spectrometer and processed with Agilent MassHunter Qualitative Analysis 8.06 software.

Preparation of nodulisporic acid E (NAE) 1 standard for LCMS and NMR spectroscopy analysis

The NAE 1 standard was prepared as described in van Dolleweerd et al 2018.² "**Large scale indole diterpene purification for NMR analysis.**" with the following modifications. NAE 1 was extracted with ethyl acetate and dry loaded onto silica for normal-phase crude purification using a chloroform and methanol gradient run through a 4 g HP 20 mm Silica column (Buchi) attached to a Reveleris X2 flash chromatography system (Buchi). The crudely purified fraction was condensed to dryness and resuspended in acetonitrile. The sample was further purified with a semi-preparative reversed phase Zorbax SB-C18 5 µm (50 × 9.4 mm) column attached to an Agilent 1260 Infinity II LC system run at a flow rate of 3.00 mL/minute and eluted with an isocratic solution of 88 % (v/v) acetonitrile containing

0.01% (v/v) formic acid. The purity of NAE 1 was assessed by LCMS and the structure was identified by NMR spectroscopy.

NMR spectroscopy

NAE 1 was prepared in deuterated chloroform. Proton (^1H), carbon (^{13}C), and 2D NMR spectra were recorded on a Jeol JNM-ECZ600R FT NMR instrument using a 600 MHz 5 mm FG/SC AutoTune SuperCOOL Open Type Probe operating for ^1H NMR at 600 MHz and 150 MHz for ^{13}C NMR. All chemical shifts are quoted on the δ -scale in ppm using residual solvent as an internal standard. ^1H and ^{13}C spectra were assigned using correlation spectroscopy (COSY), heteronuclear single quantum correlation (HSQC) spectroscopy, and heteronuclear multiple bond correlation (HMBC) spectroscopy. Spectra were acquired with Delta™ 5.2 acquisition software and processed with MestReNova processing software. All NMR spectra can be found in Table S2 and Figures S7 to S11.

Preparation of DNA constructs

DNA constructs for use in heterologous expression studies were prepared using the MIDAS cloning system as described in van Dolleweerd et al. 2018.² Accordingly, coding sequences (CDSs) of the IDT PT genes of interest were amplified (see Tables S7 for primers and S8 for synthetic genes) and cloned into the MIDAS Level-1 destination vector, pML1 (Table S9). At MIDAS Level-2, the cloned CDSs were placed under the control of heterologous promoter (ProUTR) and transcriptional terminator (UTRterm) modules to generate full-length transcription units, TUs (Table S10), which were then used to generate the multigene plasmids (Table S11).

Supplementary Tables:

Table S1. Similarity matrix for fungal aromatic prenyl transferases based on ClustalW alignment of amino acid sequences.

Enzyme & accession	PtmE	PtmD	PaxD	NodD2	NodD1	LtmF	LtmE	JanD	FtmPT1	FgaPT2	CpdNP _T	AtmD	AtaPT	AnaPT	AmyD
PtmE BAU61567	100	26.1	25.1	24.1	25.7	18.2	18.8	26.3	22.4	26.1	21.2	24.6	26.3	26.5	17.7
PtmD BAU61555	43.1	100	30.6	31.3	31.9	20.8	19.1	31.8	23.1	22	18.9	29.7	23.7	20.3	20.6
PaxD AAK11526	42	52.4	100	42.1	48	19.3	20.6	65.8	20.2	21.2	18.6	30.9	22	20.1	17.2
NodD2 AUM60055	41.7	53	61.5	100	47.6	20.1	20.4	45	22.4	22.9	19.1	31.3	22	21.2	20.7
NodD1 AUM60056	42.4	53.8	66.4	64.8	100	21.4	20.4	53.2	21.9	22.7	17.3	31.5	24.4	21.4	18.6
LtmF ABF20224	33.5	36.6	38.3	35.8	39.7	100	33.3	21.1	15.6	17.9	15.4	18.7	16.6	17.8	33.8
LtmE ABF20220*	34.2	35.3	36.7	35.9	36.8	52.3	100	21.9	18	19.9	17.7	19.3	18.7	19	55.9
JanD AGZ20478	43.2	52.3	80.6	63.1	68.5	39.9	38.9	100	22.3	22.9	17.7	30.7	24.7	21.2	20.3
FtmPT1 AAX56314	40.5	39.6	37	35.9	38.4	30.3	32.2	39	100	28.7	23.1	21.5	23.8	23.8	16.8
FgaPT2 AAX08549	42.8	39.9	38.2	40.2	39.2	32.8	34.9	39.7	45.4	100	23.5	24.4	23.7	25.2	19.6
CpdNPT ABR14712	42.1	35.2	33.3	35.1	34.8	29.3	30.1	34.2	40.7	42.1	100	17.8	21.1	25.9	19.3
AtmD CAP53937	37.7	48.8	49	49.7	49.2	34.6	33.7	50.1	34	39.4	35.1	100	21.3	19.2	18.5
AtaPT AMB20850	41.3	40.2	39.5	38.4	40.3	32.6	30.9	40.4	44.1	40.7	37.1	34.8	100	34.4	17
AnaPT EAW16181	43.2	39.1	36.8	36.2	40.3	34.2	33.7	38	43	41.6	43.5	36.2	53.1	100	19
AmyD BAO49661	33.7	36.5	32.4	35.4	35.8	51.8	71.6	34.2	29.7	32.9	33.3	32.5	31.3	37.4	100

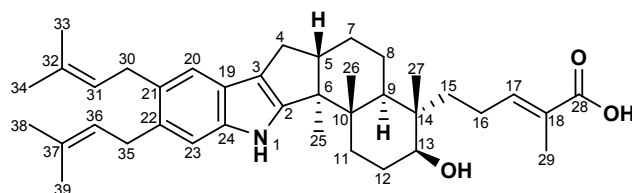
Blue shaded regions () represent % identity scores and tan shaded regions () represent % similarity scores for amino acid residues.

Alignments were made using the Gonnet similarity matrix with open gap penalty = 10.0, extend gap penalty = 0.1, delay divergent = 40%, and gap distance = 8.

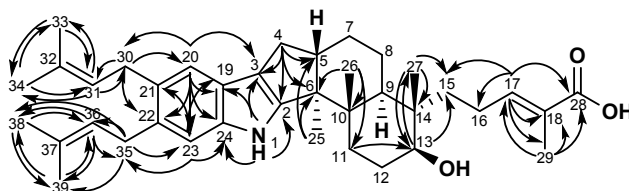
*Only the 463 C-terminal residues of LtmE were included. LtmE is a hybrid enzyme apparently formed by fusion of ancestral copies of the genes encoding LtmC and LtmF such that only C-terminus is homologous to the other aromatic PTs.³

Table S2. ^1H and ^{13}C NMR assignment of nodulisporic acid E (NAE) **1** in CDCl_3 . Spectra depicted in Figures S7 to S11 and raw spectra data can be found in the corresponding FID files.

position	NAE 1	
	^1H	^{13}C
1	7.63, brs	
2		150.32, C
3		117.92, C
4	2.63, dd, 2.28, dd	27.57, CH ₂
5	2.69, m	48.76, CH
6		53.07, C
7	1.80, m	27.64, CH ₂
8	1.59, 1.40	22.86, CH ₂
9	1.68	40.08, CH
10		39.34, C
11	1.52, 1.82	33.47, CH ₂
12		25.24, CH ₂
13	3.55, t	73.40, CH
14		41.34, C
15	1.66, 1.37	35.82, CH ₂
16	2.17 m, 2.06, m	22.61, CH ₂
17	6.89, t	144.92, CH
18		127.02, C
19		123.57, C
20	7.19, s	118.37, CH
21		131.47, C
22		132.58, C
23	7.08, s	111.50, CH
24		139.17, C
25	0.97, s	14.69, CH ₃
26	1.07, s	19.17, CH ₃
27	0.82, s	16.49, CH ₃
28		172.32, C
29	1.84, s,	12.19, CH ₃
30	3.38, 3.37 d	32.11, CH ₂
31	5.29, m	124.40, CH
32		131.42, C
33	1.73, s	25.92, CH ₃
34	1.73, s	17.97, CH ₃
35	3.37, 3.38 d	31.94, CH ₂
36	5.30, m	123.96, CH
37		131.98, C
38	1.70, s	18.01, CH ₃
39	1.74, s	25.92, CH ₃



nodulisporic acid E (NAE) **1**
 Chemical Formula: $\text{C}_{38}\text{H}_{53}\text{NO}_3$
 Exact Mass: 571.4025
 calc. $[\text{M}+\text{H}]^+$ 572.4105 m/z
 obs. $[\text{M}+\text{H}]^+$ 572.4101 m/z



Key HMBC correlations of nodulisporic acid E (NAE) **1**

Table S3. Database accession numbers for amino acid sequences of enzymes investigated in this study.

Protein	Source organism	Accession number	Reference
NodD1	<i>Hypoxylon pulvicidum</i>	AUM60056	Van de Bittner et al ¹
NodD2		AUM60055	
PaxD	<i>Penicillium paxilli</i>	AAK11526	Scott et al ⁴
JanD	<i>Penicillium janthinellum</i>	AGZ20478	Nicholson et al ⁵
PtmD	<i>Penicillium simplicissimum</i>	BAU61555	Liu et al ⁶
PtmE		BAU61567	
AtmD	<i>Aspergillus flavus</i>	CAP53937	Nicholson et al ⁷
LtmE*	Epichloe festucae var. lolii	ABF20220	Young et al ⁸
LtmF		ABF20224	
AmyD	<i>Phomopsis amygdali</i>	BAO49661	Liu et al ⁹
FgaPT2	<i>Aspergillus fumigatus</i>	AAX08549	Unsold et al ¹⁰
FtmPT1		AAX56314	Grundmann et al ¹¹
CpdNPT		ABR14712	Yin et al ¹²
AnaPT	<i>Neosartoria fischeri</i>	EAW16181	Yin et al ¹³
AtaPT	<i>Aspergillus terreus</i>	AMB20850	Chen et al ¹⁴

* LtmE is a hybrid enzyme that appears to have arisen from a fusion of the genes³ encoding LtmC (a membrane associated prenyl transferase) and LtmF (another aromatic prenyl transferase) that are both involved in the biosynthesis of indole-diterpenes. Only the X C-terminal sequences of LtmE were included as this covers the region that is homologous to other aromatic prenyl transferases.

Table S4. Table of fungal species used in this study.

<i>Penicillium paxilli</i> strain	Description	Indole-diterpene phenotype		Source ^{reference}
		NAF	Paxilline (2)	
PN2013 (ATCC®26601™)	Wild type	-	+	Barry Scott, Massey University ¹⁵
PN2250 (CY2)	PN2013/Deletion of entire <i>PAX</i> locus (ΔPAX); Hyg ^R	-	-	Barry Scott, Massey University ¹⁶
HPF1	PN2250/ <i>paxGnodCMBW::P_{trpC}-nptII-T_{trpC}</i> ; Gen ^R	+	-	In house

Table S5. Table of fungal strains generated in this study.

Description (plasmid/destination strain)	Number of transformants analysed	Notable indole-diterpene phenotype
pRC63/HPF1	10	1 monopenylylated NAF, NAE 1
pRC18/HPF1	10	NAF 2
pRC64/HPF1	10	NAF 2
pRC63/PN2013	6	2 mono- and 2 bis-prenylylated paxillines; 1 mono- and 1 bis-oxidized prenylylated paxillines
pRC18/PN2013	5	2 mono- and 2 bis-prenylylated paxillines
pRC64/PN2013	10	3 monopenylylated paxillines; 1 mono-oxidized prenylylated paxilline

Table S6. Multistep acetonitrile gradient used for LCMS analysis of fungal extracts.

Time (minutes)	% (v/v) of acetonitrile + 0.01% (v/v) formic acid
0	40
1	40
40	100
42	100

Table S7. PCR primers for amplification of transcription unit modules (TUMs).

TUM	Primer name	Primer sequence (5' to 3')
Coding Sequences (CDSs)		
<i>nodD1</i> _{CDS}	nodD1 F	cgatgta cgctctc aCTCG AATG gatgctgcttcaactcttacg
	nodD1 R2	gaccttt cgctctc tGTCTca AAGC ctactcggtatctagagatagctcg
<i>janD</i> _{CDS}	janD F1	cgatgta cgctctc aCTCG AATG gggttctcagaggtagaattg
	janD R1	gaccttt cgctctc gACCTgtctctatatgttccagattggagac
	janD F2	cgatgta cgctctc AGGTcgaccaattggagacAtcatgatcc
	janD R2	gaccttt cgctctc tGTCTca AAGC tattttatataatctcgggcacccatgtagc
<i>atmD</i> _{CDS}	atmD-F1F	cgatgta cgctctc aCTCG AATG tctactcccaagtcggataca
	atmD-F1R	aaacct cgctctc aCGTTtcaaagatgtctcggtaatccccg
	atmD-F2F	gagaca cgctctc aAAGCgtgtgttaggtttcttcagtcca
	atmD-F2R	gaccttt cgctctc tGTCTca AAGC ctacttggaaagccccttcaca
Promoter regions (ProUTRs)		
<i>trpC</i> _{ProUTR}	PtpC frag1 F	cgatgta cgctctc aCTCG GGAG gaattcatgccagttgttcccag
	PtpC frag1 R	cgatgta cgctctc aGCTTggccgactcgtg
	PtpC frag2 F	caccttt cgctctc aAAGCagacgtgaagcaggacgg
	PtpC frag2 R	cgatgt cgctctc gCAGAccattgcacaagcctc
	PtpC frag3 F	gaccttt cgctctc gTCTGcgcatggatcgtgc
	PtpC frag3 R	gaccttt cgctctc tGTCTca CATT atcgatgcttgggtagaataggtgaag
<i>janD</i> _{ProUTR}	P janD F	cgatgta cgctctc aCTCG GGAG cttaccgctccttttttctcaacg
	P janD R	gaccttt cgctctc tGTCTca CATT gtttaagatgatcttgagcttgatgaagtg
<i>janG</i> _{ProUTR}	P janG F1	cgatgta cgctctc aCTCG GGAG taacttcattaaattttcgggtactaccgctg
	P janG R1	gaccttt cgctctc gGATTgtctcgcagcgaagtggac
	P janG F2	cgatgta cgctctc aAATCcacattgcatgattgtttctattttttc
	P janG R2	gaccttt cgctctc tGTCTca CATT gtttcttcgctcgcgattgt
Terminator regions (UTRterms)		
<i>trpC</i> _{UTRterm}	T trpC frag1 F	cgatgta cgctctc aCTCG GCTT gatccacttaacgttactgaaatcatcaaac
	T trpC frag1 R	gaccttt cgctctc tCTGCttgatctcgtctgccga
	T trpC frag2 F	cgatgta cgctctc aGCAGatcaacggtcgtcaaga
	T trpC frag2 R	gaccttt cgctctc tGTCTca AGCG tctagaagaaggattacctctaaacaagtgt
<i>paxP</i> _{UTRterm}	T paxP F	cgatgta cgctctc aCTCG GCTT atagggatacgttgccggtc
	T paxP R	gaccttt cgctctc tGTCTca AGCG gagcatggattacaattttgcgag
<i>paxQ</i> _{UTRterm}	T paxQ F	cgatgta cgctctc aCTCG GCTT agggaaatttgaaatagattacactc
	T paxQ R	gaccttt cgctctc tGTCTca AGCG tctagtttcaaattcgcgtgggttg

The forward and reverse PCR primers used for amplification of TUMs (i.e. promoters (ProUTR), coding sequences (CDSs), and terminators (UTRterm)) are listed. Primers used to amplify TUM fragments for domestication purposes (i.e. removal of internal sites for *AarI*, *BsaI* or *BsmBI*) are shaded in orange (■). The template for amplification of *nod* CDSs was genomic DNA from *Hypoxylon pulicidum* strain ATCC® 74245TM.¹⁷ The template for amplification of *pax* gene TUMs was genomic DNA from *Penicillium paxilli* strain ATCC® 26601TM (PN2013) [Accession HM171111].¹⁵ The template for amplification of *jan* gene TUMs was genomic DNA from *Penicillium janthinellum* strain PN2408 [Accession AGZ20478.1]. The template for amplification of *atm* gene TUMs was genomic DNA from *Aspergillus flavus* strain NRRL6541 [Accession CAP53937.2]. The PCR products used to produce the *trpC*_{ProUTR} module and *trpC*_{UTRterm} module were amplified from plasmid pII99.¹⁸ The *BsmBI* recognition sites are colour coded (cgctctc), with the overhangs generated following *BsmBI* cleavage shown by the grey shading (■). The 5' (prefix)

and 3' (suffix) nucleotide bases, which flank each TUM and form the basis of the address system for each of the MIDAS modules, are shown in blue and red respectively.

Table S8. Synthetic gene sequence for nourseothricin resistance gene (*natR*).

TUM	
Synthetic gene sequence	
Modified Coding Sequence (CDS)	
<i>natR</i> _{CDS}	<p>cgatgtacgtctcaCTCGAATGaccactcttgacgacacggcttaccgtaccacatgtcccggggacgccgaggccatcgaggcac tggatgggtccttcaccaccgacaccgtcttccgctcaccgccaccggggacggcttaccctgcgggaggtgccggtggacccgccct gaccaaggtgttccccgacgacgaaagegacgacgaatcggacgccggggaggatggcgaccggactccggacgttcgtcgcgtacg gggacgacggcgacctggcgggcttctggttgtctcgtactccggctggaaccgccggctgaccgtcgaggacatcgaggtegccccgg agcaccg gggcacggggtcgggaga gcgttgatggggctcgcgactgagttcgtcgcgagcagggcggggcacctctggctggag gtcaccaacgtcaacgcaccggcgatccacgcgtaccggcgatggggttcacctctgcggcctggacaccgccctgtacgacggcacc gcctcggacggcgagcagggcgtctacatgagcatgccctgccctgaGCTTgAGACagagacgaaagtc</p>

The *natR*_{CDS} module (conferring resistance to nourseothricin) was generated as a synthetic gene based on the *Streptomyces noursei* nourseothricin acetyltransferase coding sequence (GenBank: X73149.1) with MIDAS restriction sites added to the 5' and 3' ends, and some codon optimisation (modified bases shown in grey). One internal *BsmBI* cut site was removed at position 300 by substituting a G for a T (shown in pink). The *BsmBI* recognition sites are colour coded (cgctctc), with the overhangs generated following *BsmBI* cleavage shown by the grey shading (■). The 5' (prefix) and 3' (suffix) nucleotide bases, which flank each TUM and form the basis of the address system for each of the MIDAS modules, are shown in blue and red respectively.

Table S9. MIDAS Level-1 plasmid library: Assembly of TUMs in pML1.

[GGAG]		[AATG]	[GCTT]	[CGCT]	
ProUTR modules		CDS modules		UTRterm modules	
Plasmid name	Description	Plasmid name	Description	Plasmid name	Description
pSK17	<i>trpC</i> _{ProUTR}	pRC1	<i>natR</i> _{CDS}	pSK15	<i>trpC</i> _{UTRterm}
pLB9	<i>janD</i> _{ProUTR}	pRC25	<i>nodD1</i> _{CDS}	pSK70	<i>paxP</i> _{UTRterm}
pLB1	<i>janG</i> _{ProUTR}	pLB10	<i>janD</i> _{CDS}	pSK72	<i>paxQ</i> _{UTRterm}
		pMN4	<i>atmD</i> _{CDS}		

This table represents the MIDAS level-1 TUMs that were used to assemble MIDAS level-2 TUs (Table S10). The 4 base prefixes and suffixes (5' to 3') that flank each TUM are shown at the top of the table to highlight the sequences used to bind the TUMs together to make MIDAS level-2 TUs. These 4 base flanking regions are depicted in the primer table (Table S8) in blue (forward addresses) and red (reverse addresses).

Table S10. MIDAS Level-2 plasmid library: Assembly of TUs in pML2 destination vectors.

TU	Level-1 entry clones used for TU assembly			pML2 destination vector	Level-2 entry clones	
	ProUTR	CDS	UTRterm		Name	Description
<i>natR</i>	pSK17	pRC1	pSK15	pML2(+)WF	pRC2	(<i>P_{trpC}-natR-T_{trpC}</i>)▶:pML2(+)WF
<i>nodD1</i>	pLB9	pRC25	pSK70	pML2(+)WR	pRC47	(<i>P_{janD}-nodD1-T_{paxP}</i>)▶:pML2(+)BF
<i>janD</i>		pLB10		pML2(+)BR	pKV141	(<i>P_{janD}-janD-T_{paxP}</i>)▶:pML2(+)BF
<i>atmD</i>	pLB1	pMN4	pSK72	pML2(+)WR	pRC54	(<i>P_{janG}-atmD-T_{paxQ}</i>)▶:pML2(+)BF

This table represents the construction of the MIDAS level-2 TUs that were used to assemble MIDAS level-3 multi-gene plasmids (Table S11) for heterologous expression studies. TUs are described by the CDS they contain (in the TU column) and the Level-1 entry clones used for TU assembly are depicted in their corresponding ProUTR, CDS, or UTRterm columns. The column labeled pML2 destination vector describes the type of MIDAS Level-2 plasmid that was used to assemble each TU. The names of the Level-2 entry plasmids produced are shown in the blue shaded (■) column and the TU orientation, determined by the pML2 destination vector, is shown by the arrowhead (▶ for forward (F) destination vector) in the Level-2 entry clone **description**.

Table S11. MIDAS Level-3 plasmid library: Multigene assemblies in pML3.

Step	Level-2 entry clone		Destination vector	Golden Gate reaction	Product Level-3 plasmid		
	Name	Description			Name	Description	Plasmid size (kb)
1	pRC2	(<i>P_{trpC}-natR-T_{trpC}</i>)▶:pML2(+) <i>WF</i>	pML3	<i>AarI</i>	pRC3	pML3: <i>natR</i> ▶	5.3
2	pRC47	(<i>P_{janD}-nodD1-T_{paxP}</i>)▶:pML2(+) <i>BF</i>	pRC3	<i>BsmBI</i>	pRC63	pML3: <i>natR</i> ▶: <i>nodD1</i> ▶	8.4
2	pKV141	(<i>P_{janD}-janD-T_{paxP}</i>)▶:pML2(+) <i>BF</i>	pRC3	<i>BsmBI</i>	pRC18	pML3: <i>natR</i> ▶: <i>janD</i> ▶	8.3
2	pRC54	(<i>P_{janG}-atmD-T_{paxQ}</i>)▶:pML2(+) <i>BF</i>	pRC3	<i>BsmBI</i>	pRC64	pML3: <i>natR</i> ▶: <i>atmD</i> ▶	8.7

This table shows the Level-2 entry clone and Level-3 destination vectors used to construct the Level-3 product plasmids. The number of level 3 assembly reactions used to create the level-3 plasmid is indicated by number in the step column. The name and description of each Level-2 entry clone and the Level-3 destination vector that the Level-2 entry clones were assembled into are shown in their respective columns. The enzyme (*AarI* or *BsmBI*) used to mediate the Level-3 reaction is listed in the Golden Gate reaction column. The name (blue shaded (■) column), description and size of plasmids produced during each cycle of Level-3 assembly are shown in their respective Level-3 product plasmid columns. In the Level-3 product plasmid descriptions, TUs are annotated with the name of the CDS they contain, and TU orientation is shown by the arrowhead.

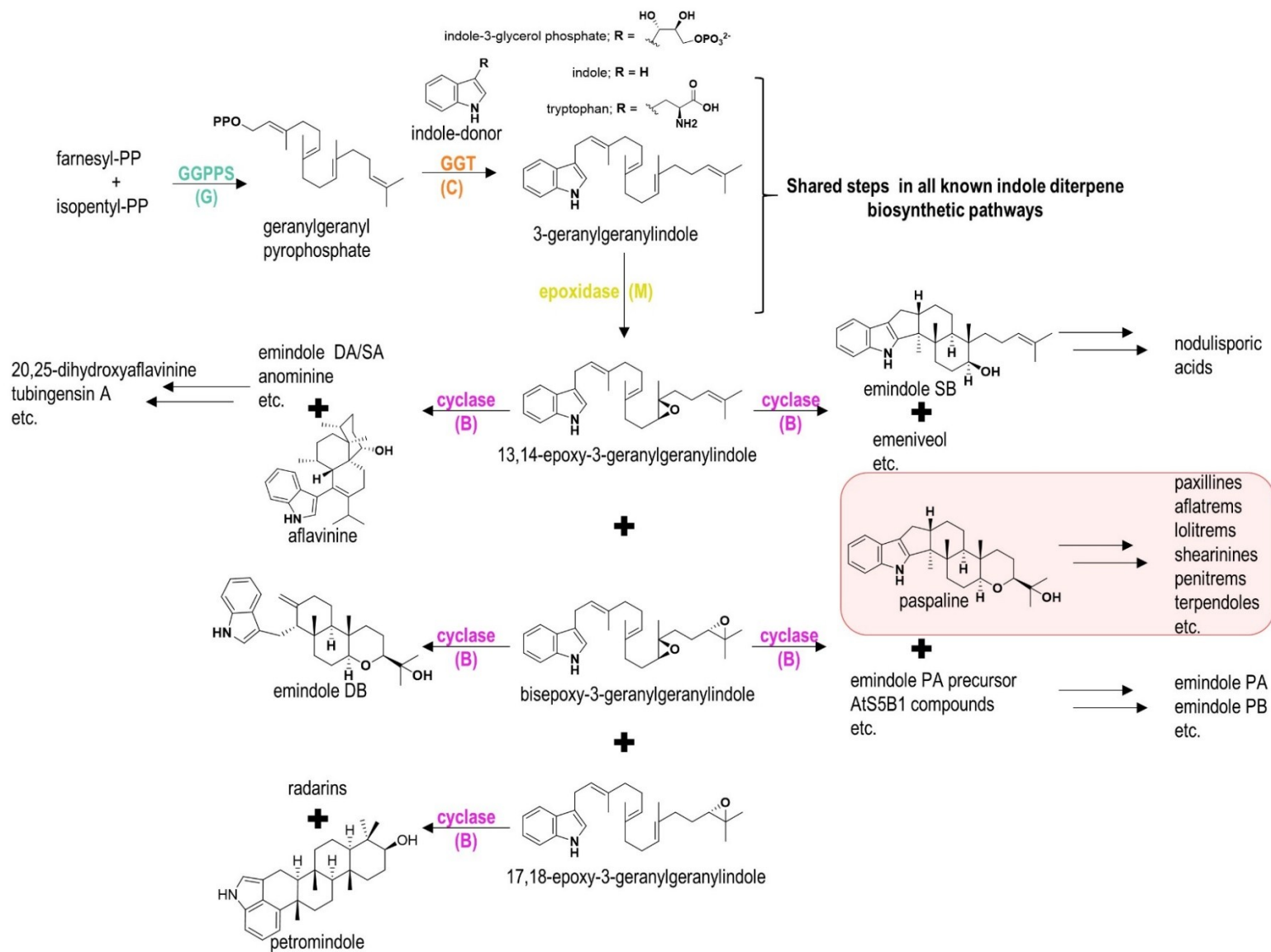


Figure S1. Secondary-metabolic steps in the biosynthetic pathway of IDTs that give rise to the diverse IDT structures. Arrows represent enzymatic steps in IDT biosynthesis and the enzyme colour corresponds to the number of the specific step in the pathway. The biosynthetic pathways for paspaline-derived IDTs, for which all previously characterized IDT PTs belong to, is highlighted with the red box.

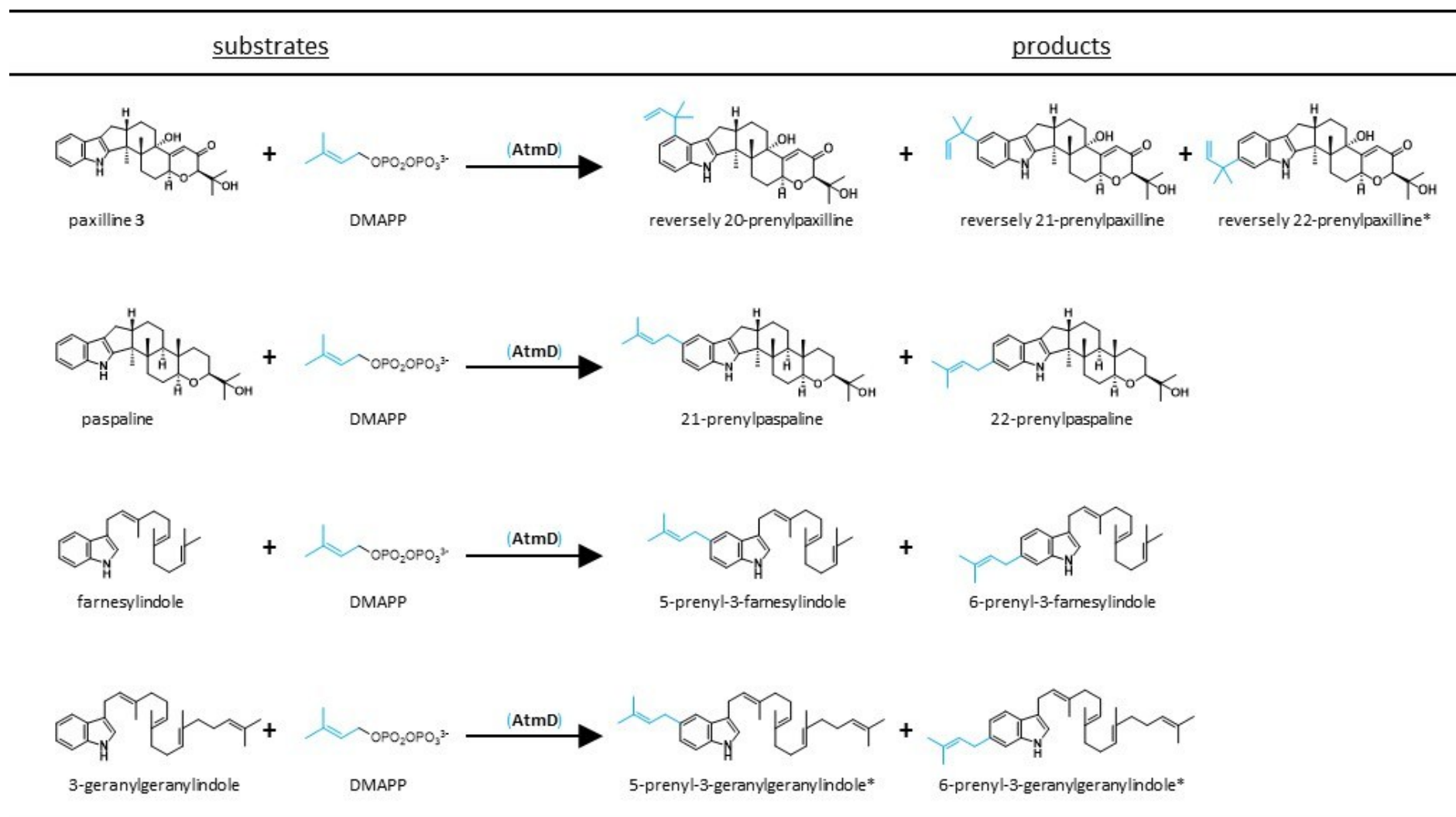


Figure S2. Depiction of AtmD substrate promiscuity tested by Liu et al 2013¹⁹ using *in vitro* feeding experiments. Theoretical minor products are indicated by and asterisk (*).

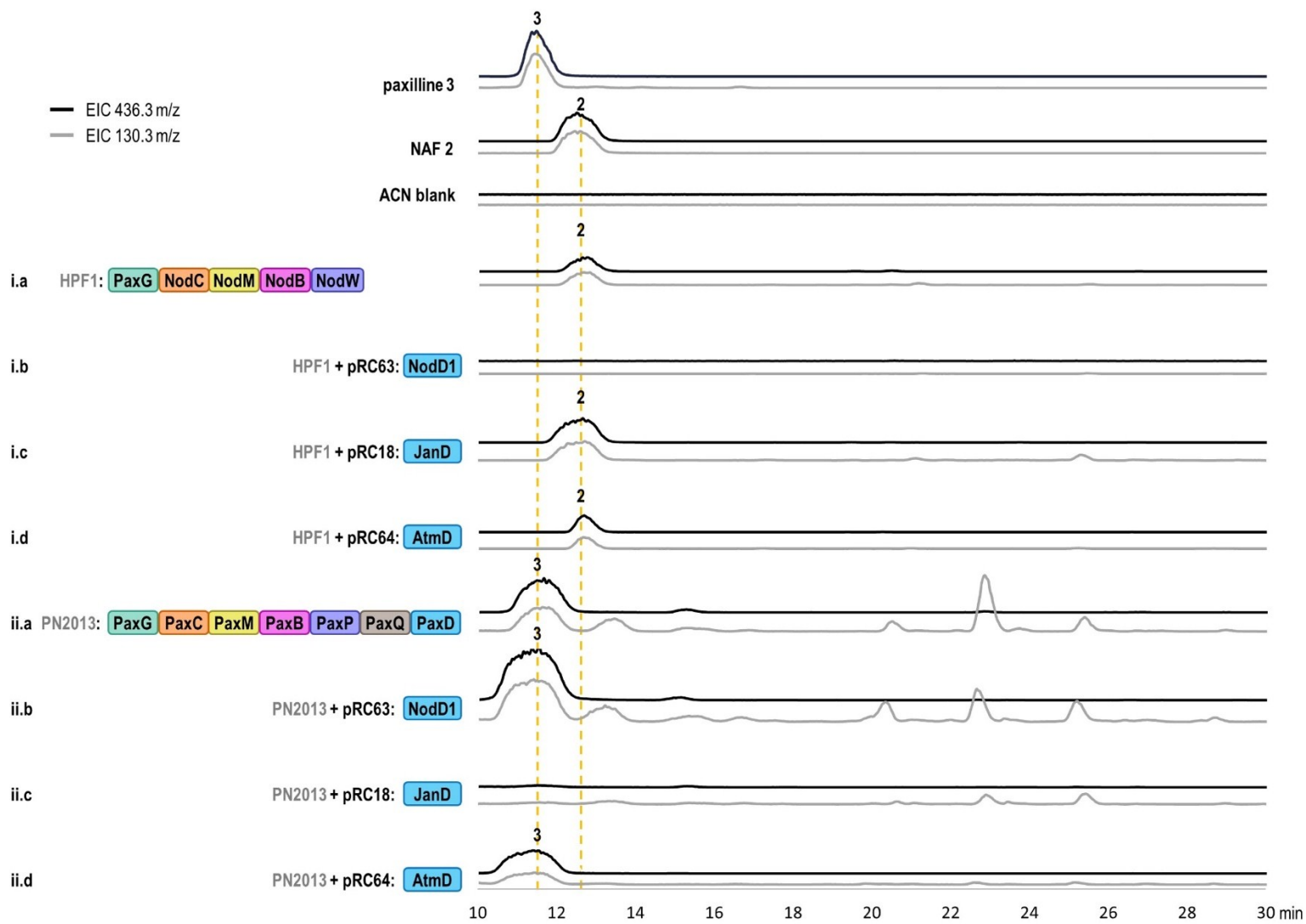


Figure S3. Extracted ion chromatograms (EICs) used to detect paxilline 3 (11.3 minutes, $[M+H]^+$ 436.3 m/z) and NAF 2 (12.6 minutes, $[M+H]^+$ 436.3 m/z). The 130.3 m/z EIC is used to confirm the presence of a nonprenylated IDT. Fragmentation energies of 100 V and 200 V were used to capture the 436.3 m/z and 130.3 m/z EICs, respectively. All 436.3 m/z and 130.3 m/z EICs have been scaled to 1,100,000 AU and 600,000 AU, respectively.

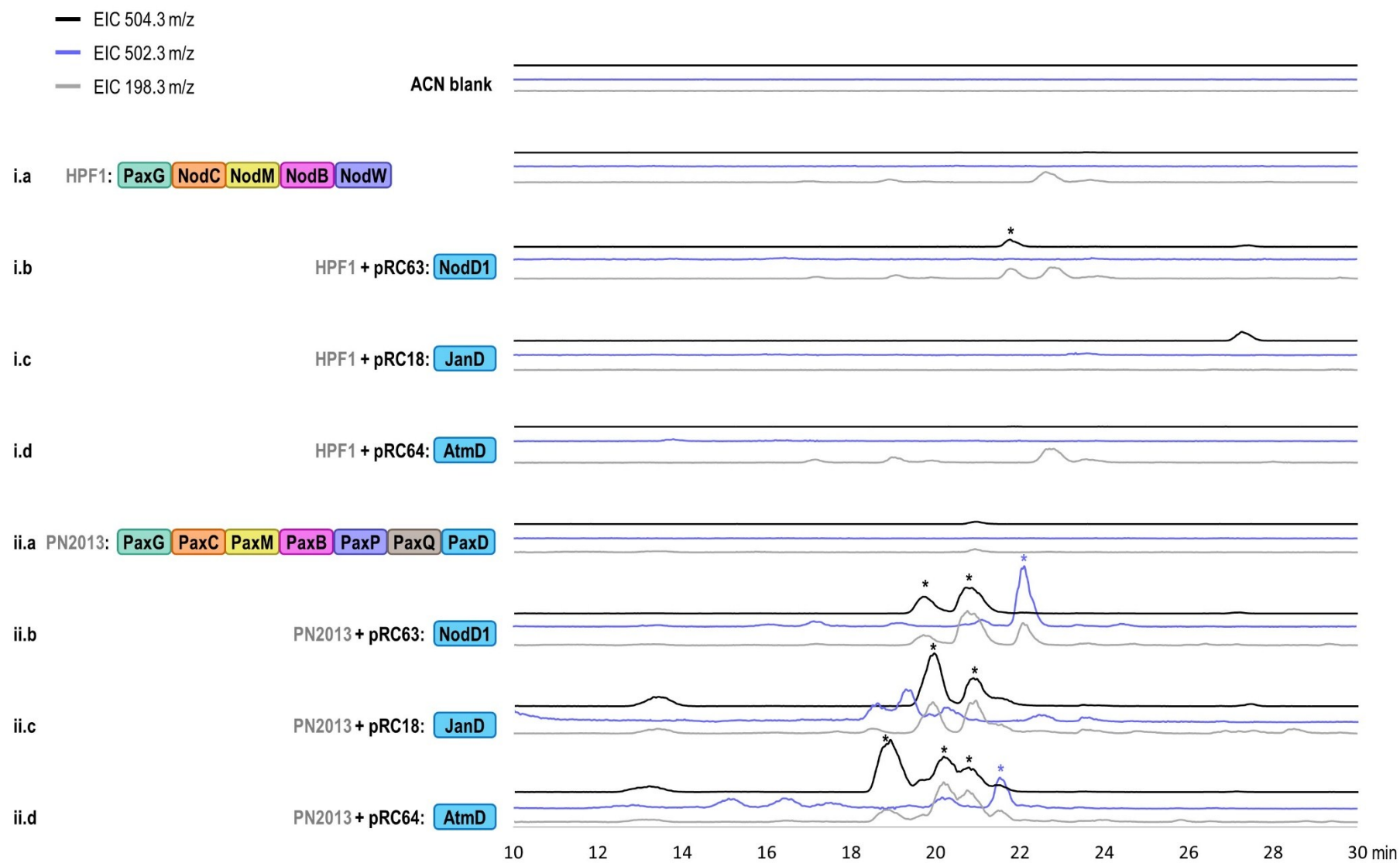


Figure S4. Extracted ion chromatograms (EICs) used to detect monoprenylated products. The 504.3 m/z EICs correspond to paxilline 3 or NAF 2 that contain a single prenyl group, the 502.3 m/z EICs correspond to an oxidized form (i.e. -2H) of the monoprenylated products, and the 198.3 m/z EICs correspond to the major ion fragment of monoprenylated paxilline or NAF. Fragmentation energies of 100 V was used to capture the 504.3 m/z and 502.3 m/z EICs, and a fragmentation energy of 200 V was used to capture the 198.3 m/z EICs. All 504.2

m/z, 502.4 *m/z* and 198.3 *m/z* EICs have been scaled to 700,000 AU, 140,000 AU, and 200,000 AU, respectively. Novel monoprenylated compounds, not present in parental strains, are indicated by an asterisks (*).

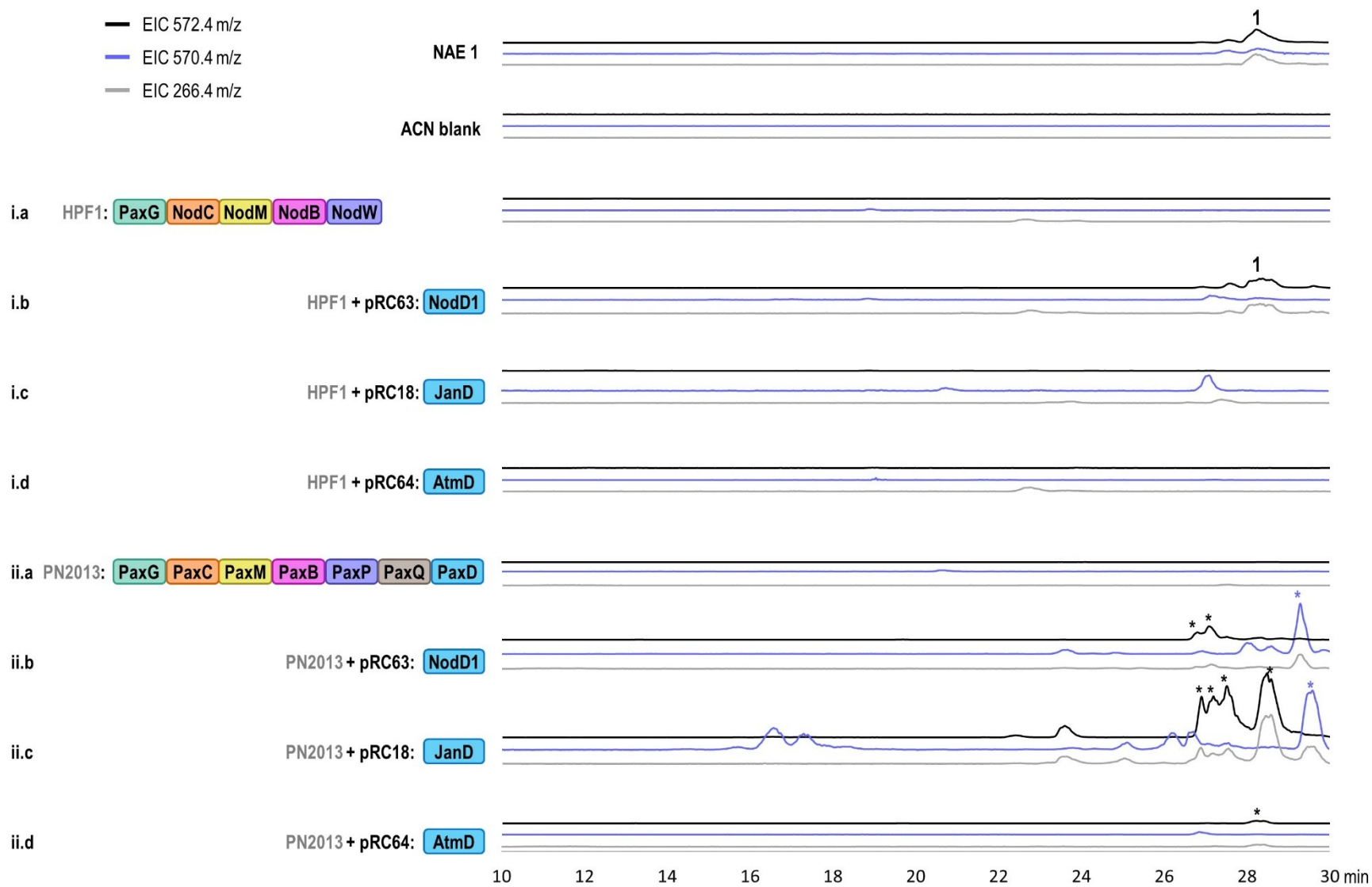


Figure S5. Extracted ion chromatograms (EICs) used to detect bisprenylated products. The 572.4 m/z EICs correspond to paxilline 3 or NAF 2 that contain a two prenyl groups, the 570.4 m/z EICs correspond to an oxidized form (i.e. -2H) of the bisprenylated products, and the 266.4 m/z EICs correspond to the major ion fragment of bisprenylated paxilline or NAF. Fragmentation energies of 100 V was used to capture the 572.4 m/z and 570.4 m/z EICs, and a fragmentation energy of 200 V was used to capture the 266.4 m/z EICs. All 572.4

m/z, 570.4 *m/z* and 266.4 *m/z* EICs have been scaled to 1,400,000 AU, 350,000 AU, and 350,000 AU, respectively. Novel bisprenylated compounds, not present in parental strains, are indicated by an asterisks (*).

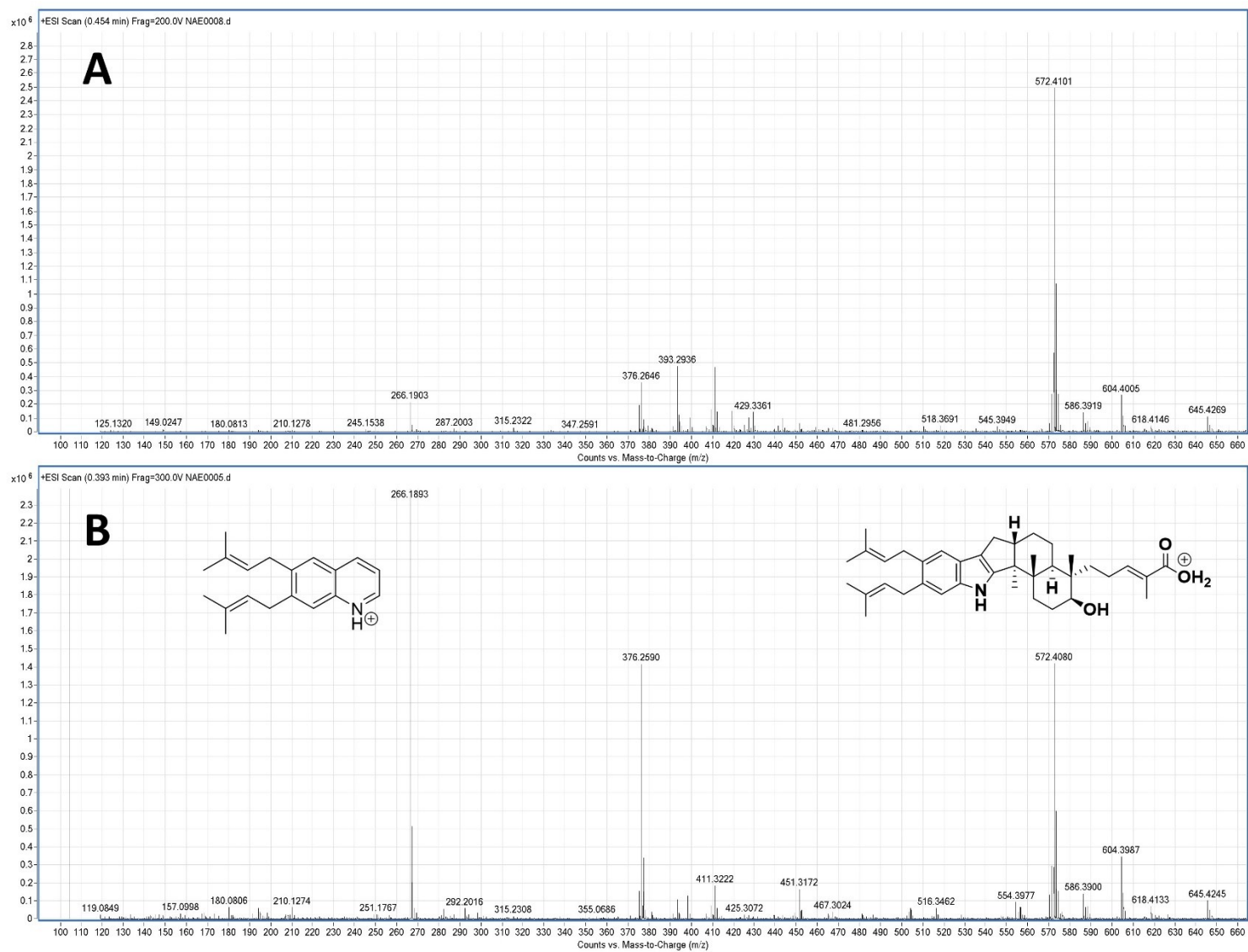


Figure S6. High-Resolution Mass Spectrometry (HRMS) results for NAE 1 characterization. A depicts the HRMS of NAE 1 with a fragmentation energy of 200 V showing the $[M+H]^+$ parent ion at 572.4101 m/z and B shows the HRMS of NAE 1 with a fragmentation energy of 300 V showing the fragmentation of the $[M+H]^+$ parent ion at 572.4080 m/z to the key bisprenylated IDT $[M+H]^+$ ion of 266.1893 m/z .

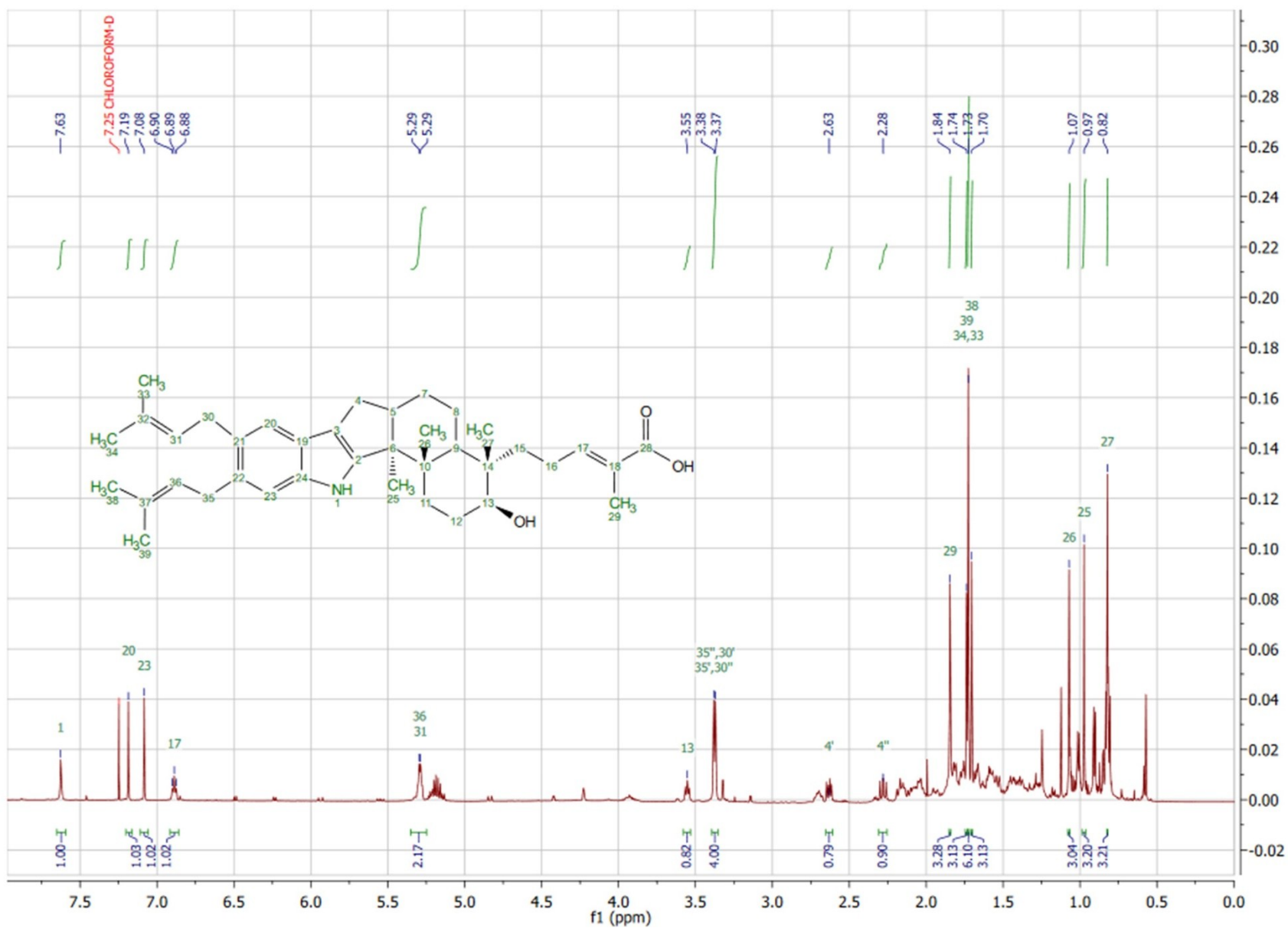


Figure S7. ¹H-NMR spectra for NAE 1 standard in CDCl₃ at 600 MHz.

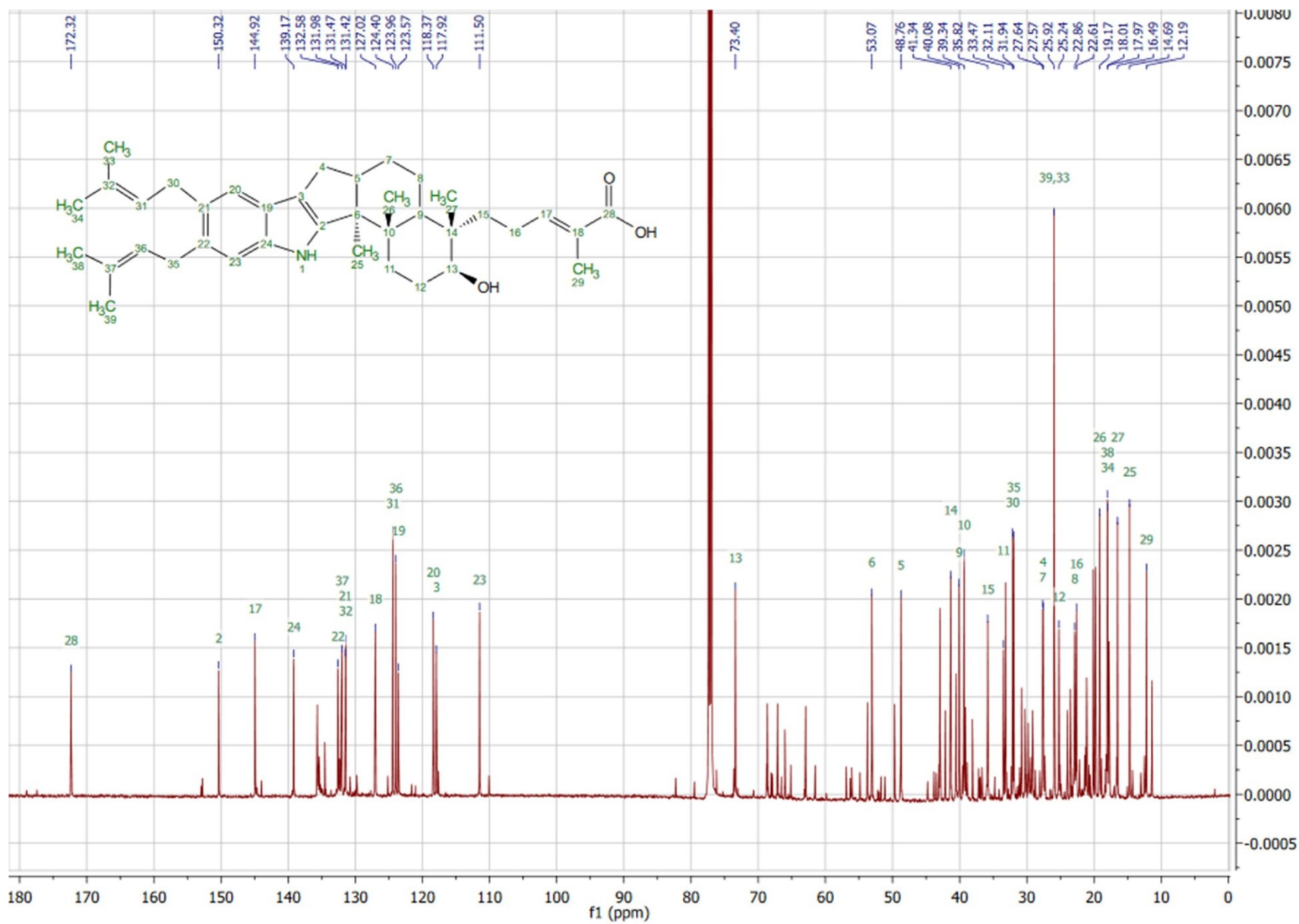


Figure S8. ^{13}C -NMR spectra for NAE 1 standard in CDCl_3 at 150 MHz.

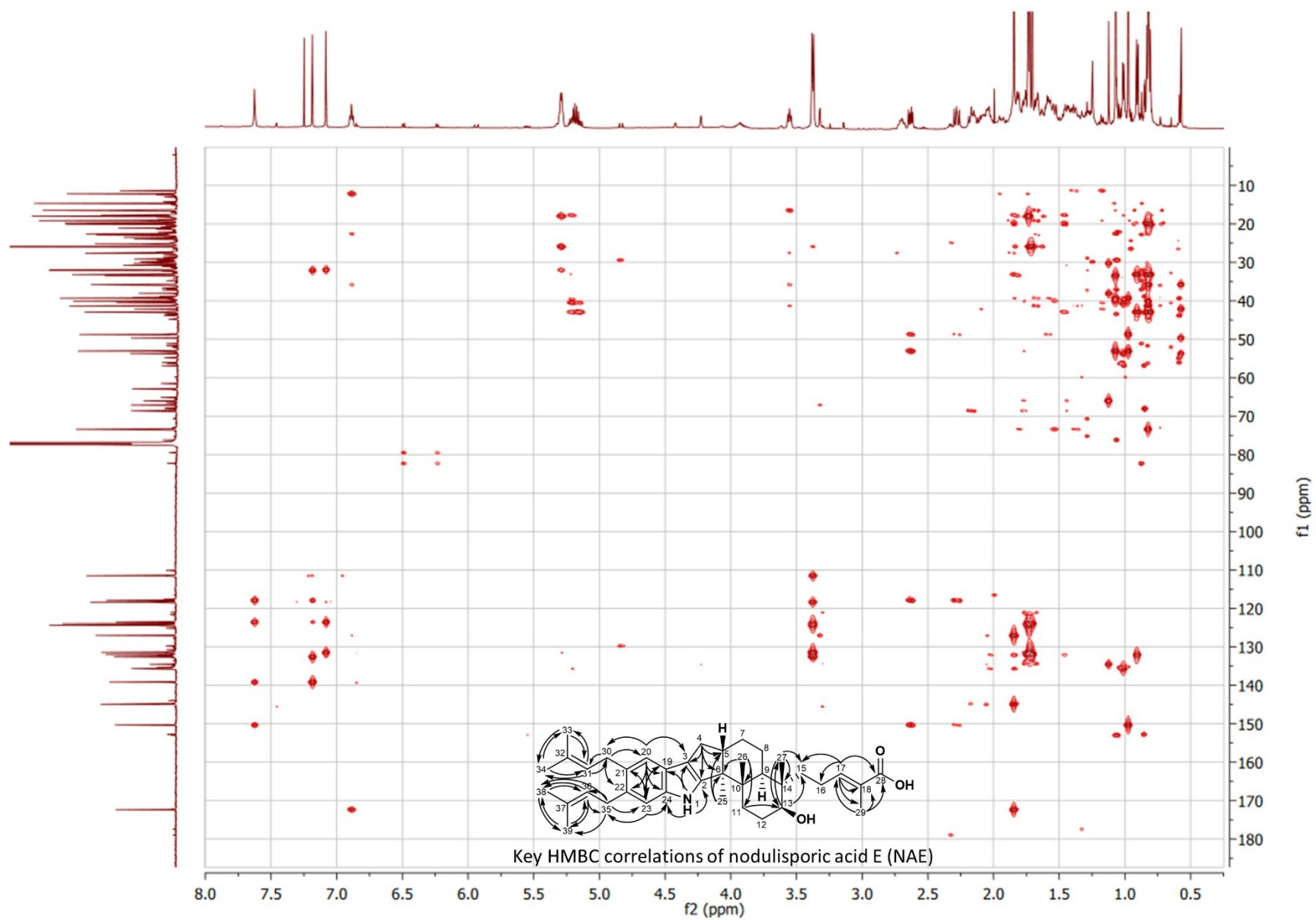


Figure S9. HMBC-NMR spectra for NAE 1 standard in CDCl₃ at 600 MHz.

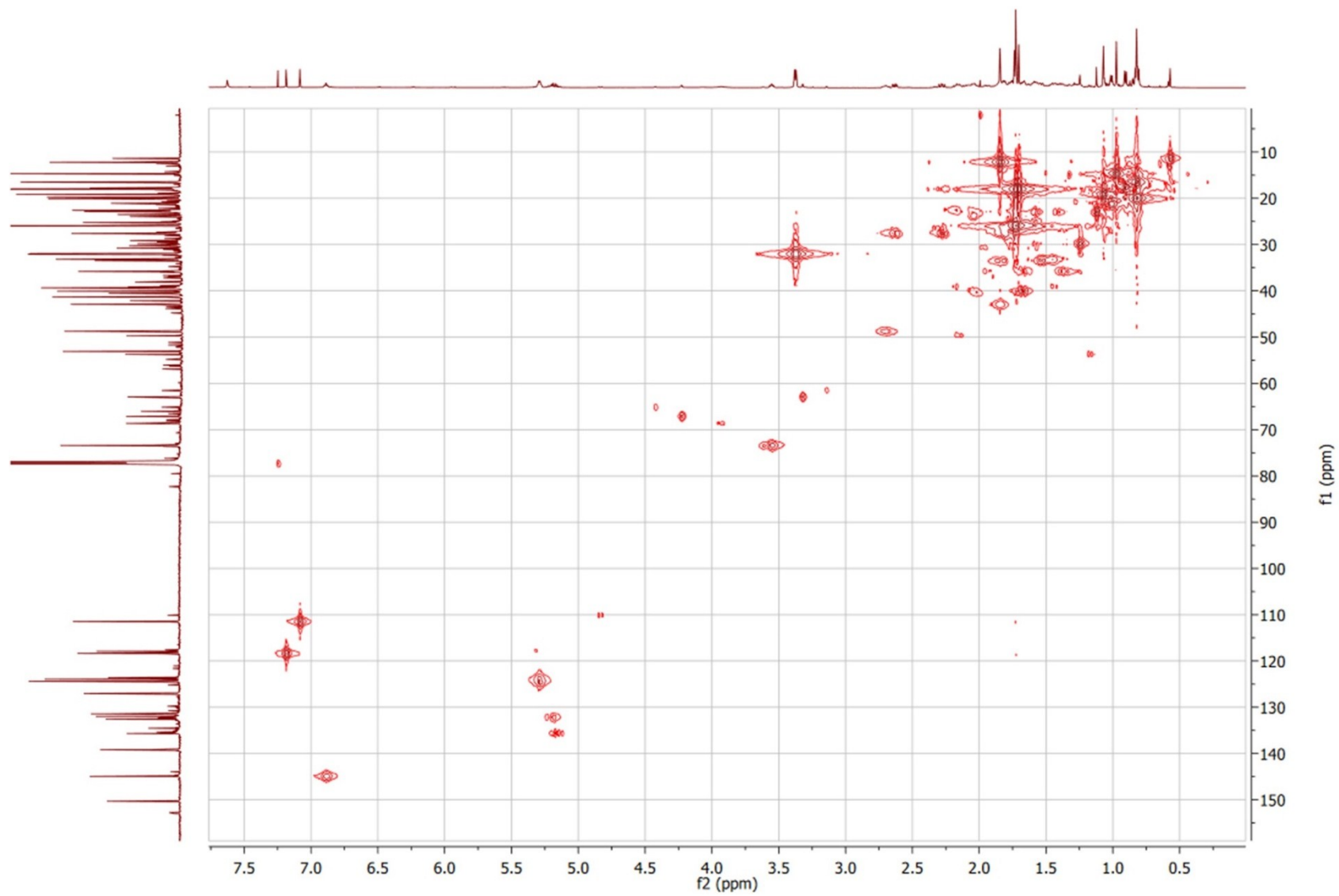


Figure S11. HMQC-NMR spectra for NAE 1 standard in CDCl_3 at 600 MHz.

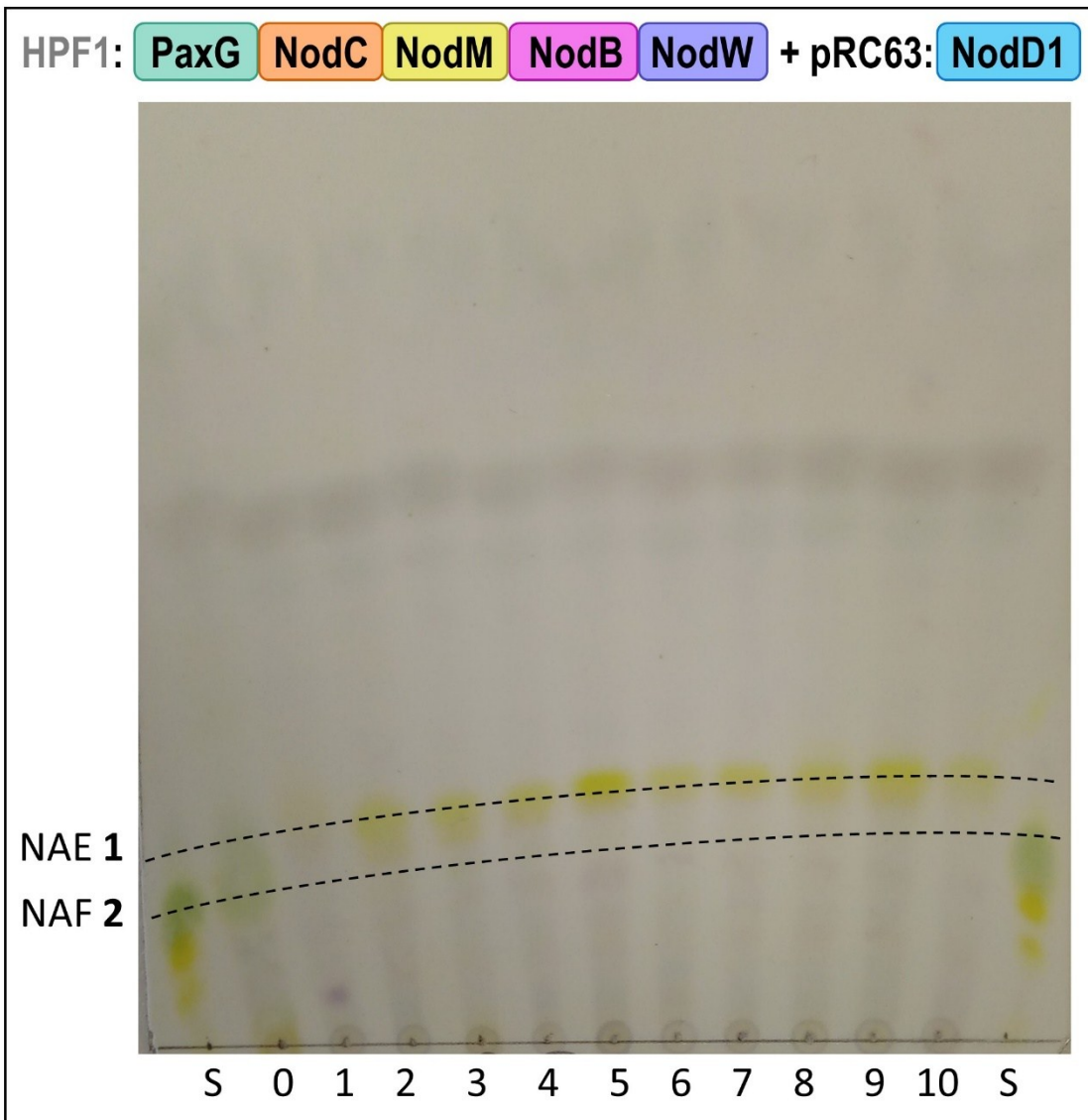


Figure S12. TLC of ten HPF1:pRC63 (*nodD1*) transformant extracts. Lanes: S = NAF 2, 0 = HPF1 + pRC13 (non-NAE producing strain), 1-10 = HPF1:pRC63 (*nodD1*) transformants. NAF 2 is identified by a green spot on the TLC plate and NAE 1 is identified by a yellow spot on the TLC plate. This TLC indicates that NAE 1 is present in at least nine of ten transformants (lanes 2 to 10).

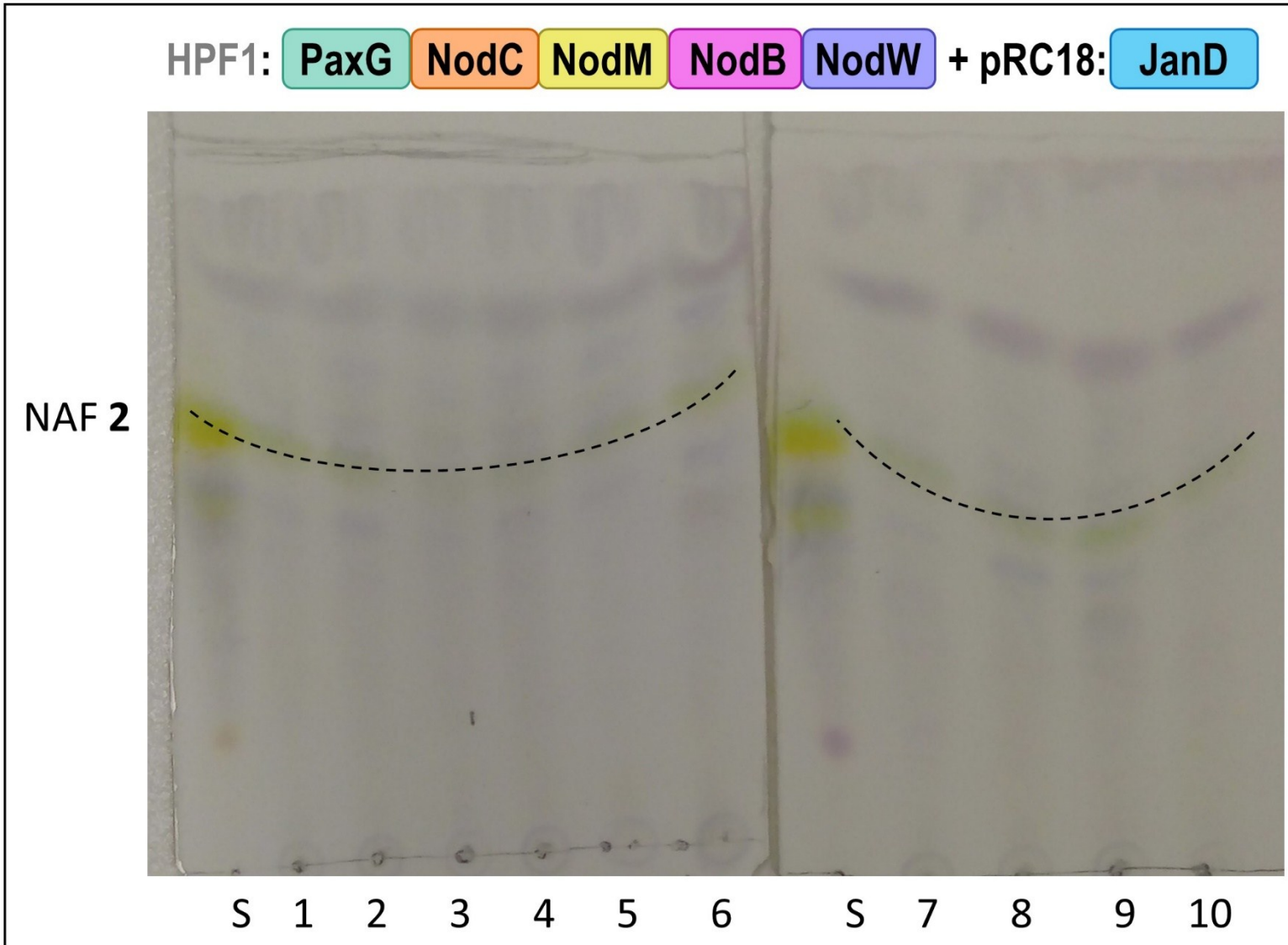


Figure S13. TLC of ten HPF1:pRC18 (*janD*) transformant extracts. Lanes: S = NAF 2, 1-10 = HPF1:pRC18 (*janD*) transformants. NAF 2 is identified by a green spot on the TLC plate. No new prenylated IDTs were detected in any of the ten transformant extracts by TLC or LC-MS analysis.

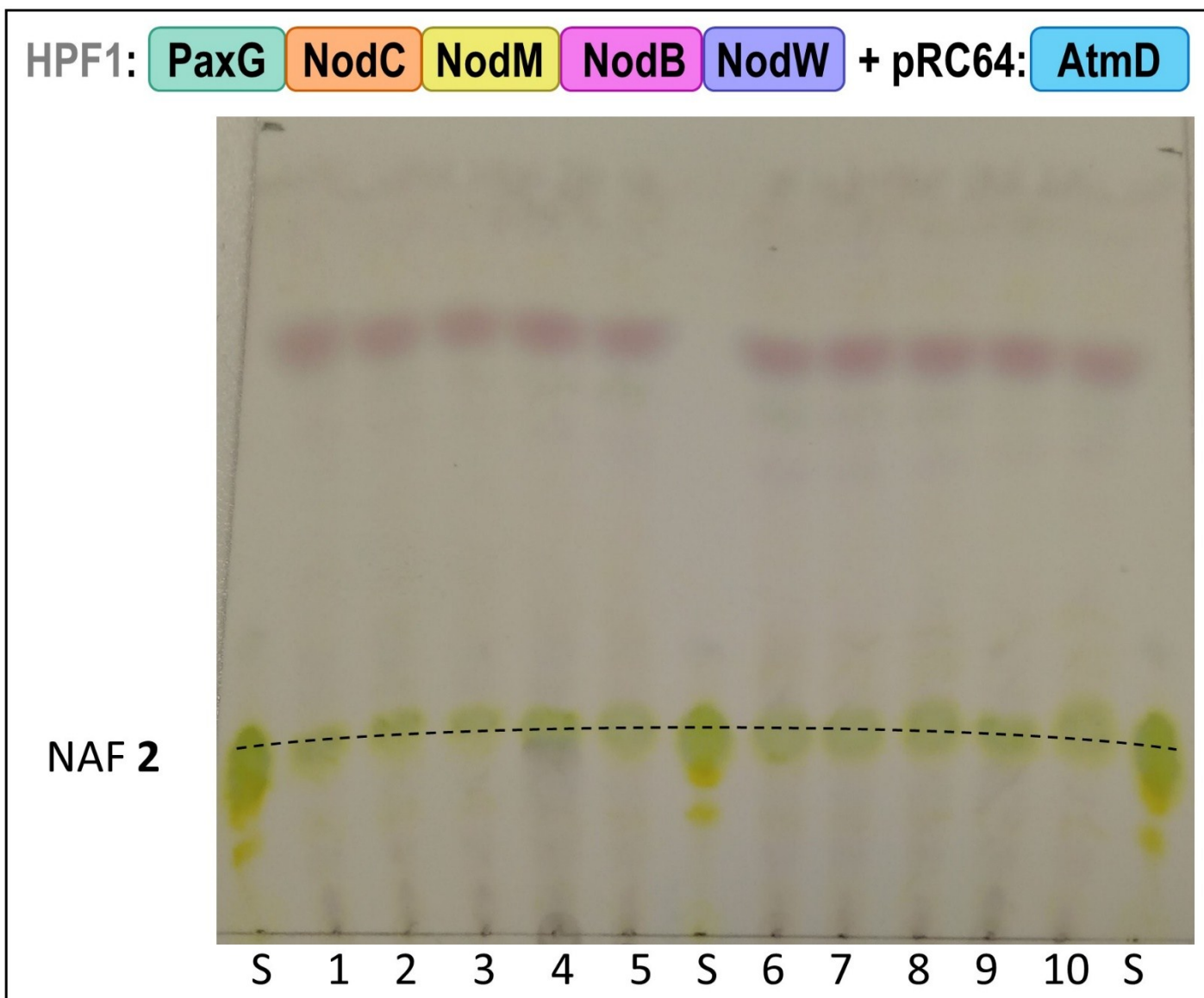


Figure S14. TLC of HPF1:pRC64 (*atmD*) transformant extracts. Lanes: S = NAF 2, 1-10 = HPF1:pRC64 (*atmD*) transformants. NAF 2 is identified by a green spot on the TLC plate. No new prenylated IDTs were detected in any of the ten transformant extracts by TLC or LC-MS analysis.

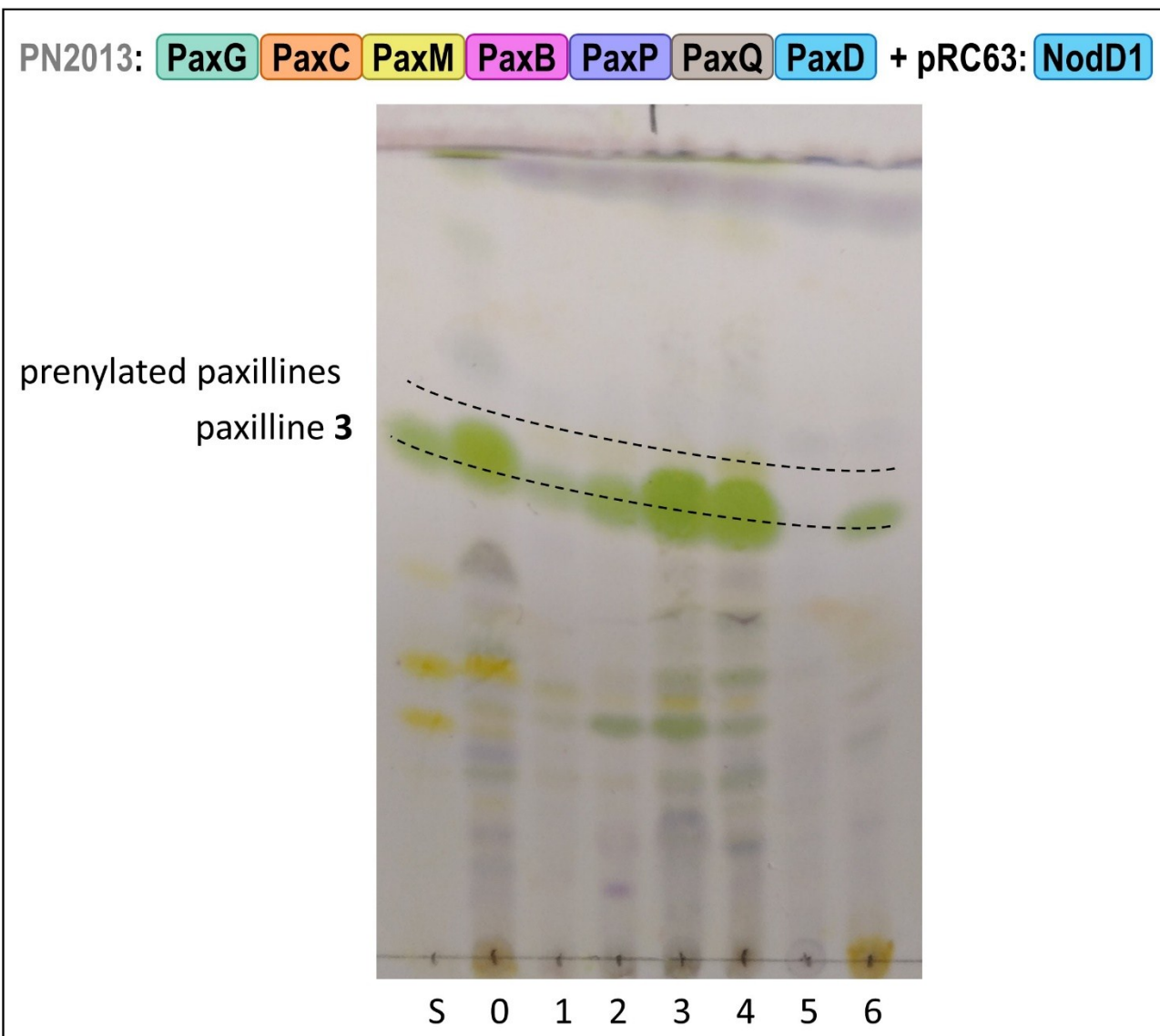


Figure S15. TLC of six PN2013:pRC63 (*nodD1*) transformant extracts. Lanes: S = paxilline 3, 0 = PN2013 (wildtype *P. paxilli* that does not produce detectable prenylated products), 1-6 = PN2013:pRC63 (*nodD1*) transformants. Paxilline 3 is identified by a green spot on the TLC plate and prenylated paxillines are identified by a yellow spot on the TLC plate. This TLC indicates that prenylated paxillines are present in at least two of six transformants (lanes 3 and 4).

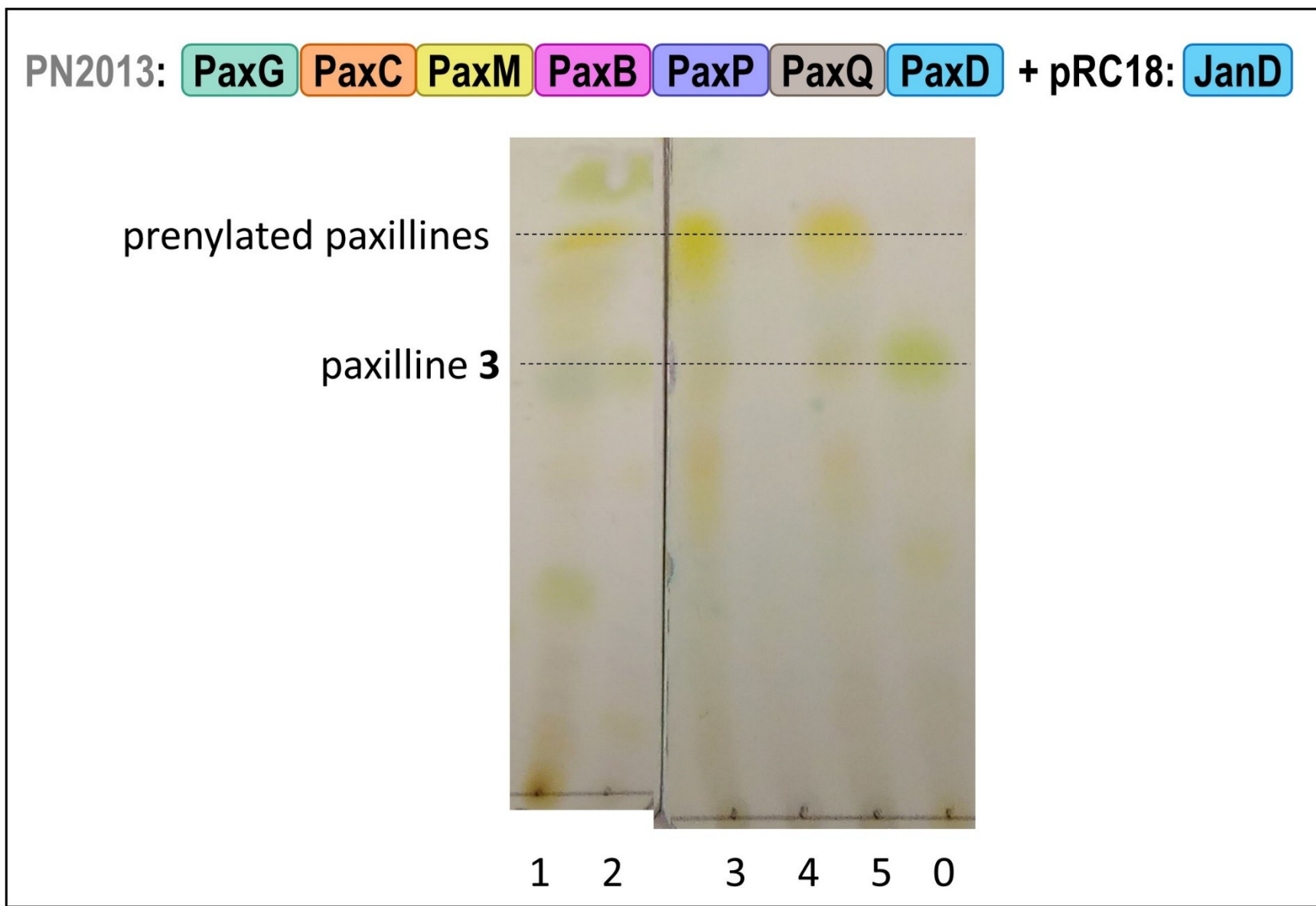


Figure S16. TLC of five PN2013:pRC18 (*janD*) transformant extracts. Lanes: 0 = PN2013 (wildtype *P. paxilli*), 1-5 = PN2013:pRC18 (*janD*) transformants. Paxilline 3 is identified by a green spot on the TLC plate and prenylated paxillines are identified by a yellow spot on the TLC plate. This TLC indicates that prenylated paxillines are present in at least three of five transformants (lanes 1, 3 and 5).

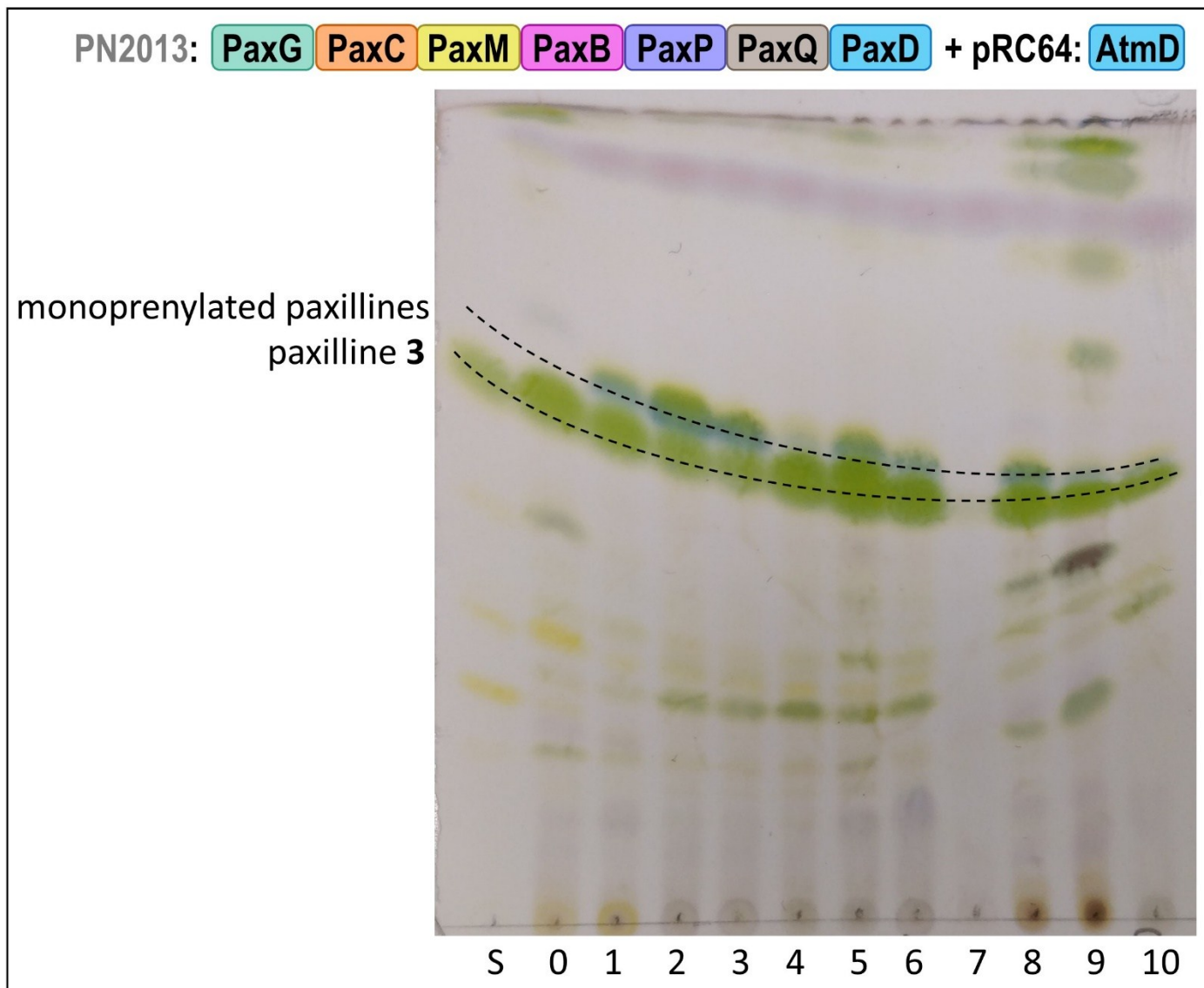


Figure S17. TLC of ten PN2013:pRC64 (*atmD*) transformant extracts. Lanes: S = paxilline 3, 0 = PN2013 (wildtype *P. paxilli*), 1-10 = PN2013:pRC64 (*atmD*) transformants. Paxilline 3 is identified by a green spot on the TLC plate and monoprenylated paxillines are identified by a blue spot on the TLC plate. This TLC indicates that monoprenylated paxillines are present in at least seven of ten transformants (lanes 1, 2, 3, 5, 6, 8 and 9).

Supplementary References

1. K. C. Van de Bittner, M. J. Nicholson, L. Y. Bustamante, S. A. Kessans, A. Ram, C. J. van Dolleweerd, B. Scott and E. J. Parker, *J. Am. Chem. Soc.*, 2018, 140, 582-585.
2. C. J. van Dolleweerd, S. A. Kessans, K. C. Van de Bittner, L. Y. Bustamante, R. Bundela, B. Scott, M. J. Nicholson and E. J. Parker, *ACS Synthetic Biology*, 2018, 7, 1018-1029.
3. C. L. Schardl, C. A. Young, U. Hesse, S. G. Amyotte, K. Andreeva, P. J. Calie, D. J. Fleetwood, D. C. Haws, N. Moore, B. Oeser, D. G. Panaccione, K. K. Schweri, C. R. Voisey, M. L. Farman, J. W. Jaromczyk, B. A. Roe, D. M. O'Sullivan, B. Scott, P. Tudzynski, Z. An, E. G. Arnaoudova, C. T. Bullock, N. D. Charlton, L. Chen, M. Cox, R. D. Dinkins, S. Florea, A. E. Glenn, A. Gordon, U. Guldener, D. R. Harris, W. Hollin, J. Jaromczyk, R. D. Johnson, A. K. Khan, E. Leistner, A. Leuchtman, C. Li, J. Liu, J. Liu, M. Liu, W. Mace, C. Machado, P. Nagabhyru, J. Pan, J. Schmid, K. Sugawara, U. Steiner, J. E. Takach, E. Tanaka, J. S. Webb, E. V. Wilson, J. L. Wiseman, R. Yoshida and Z. Zeng, *PLoS Genet*, 2013, 9, e1003323.
4. B. Scott, C. A. Young, S. Saikia, L. K. McMillan, B. J. Monahan, A. Koulman, J. Astin, C. J. Eaton, A. Bryant, R. E. Wrenn, S. C. Finch, B. A. Tapper, E. J. Parker and G. B. Jameson, *Toxins*, 2013, 5, 1422-1446.
5. M. J. Nicholson, C. J. Eaton, C. Stärkel, B. A. Tapper, M. P. Cox and B. Scott, *Toxins*, 2015, 7, 2701-2722.
6. C. Liu, K. Tagami, A. Minami, T. Matsumoto, J. C. Frisvad, H. Suzuki, J. Ishikawa, K. Gomi and H. Oikawa, *Angew. Chem. Int. Ed.*, 2015, 54, 5748-5752.
7. M. J. Nicholson, A. Koulman, B. J. Monahan, B. L. Pritchard, G. A. Payne and B. Scott, *Applied and Environmental Microbiology*, 2009, 75, 7469-7481.
8. C. A. Young, S. Felitti, K. Shields, G. Spangenberg, R. D. Johnson, G. T. Bryan, S. Saikia and B. Scott, *Fungal Genet. Biol.*, 2006, 43, 679-693.
9. C. Liu, M. Noike, A. Minami, H. Oikawa and T. Dairi, *Biosci., Biotechnol., Biochem.*, 2014, 78, 448-454.
10. I. A. Unsold, *Microbiology*, 2005, 151, 1499-1505.
11. A. Grundmann and S. M. Li, *Microbiology*, 2005, 151, 2199-2207.
12. W. B. Yin, H. L. Ruan, L. Westrich, A. Grundmann and S. M. Li, *ChemBioChem*, 2007, 8, 1154-1161.
13. W.-B. Yin, X.-L. Xie, M. Matuschek and S.-M. Li, *Org. Biomol. Chem.*, 2010, 8.
14. R. Chen, B. Gao, X. Liu, F. Ruan, Y. Zhang, J. Lou, K. Feng, C. Wunsch, S. M. Li, J. Dai and F. Sun, *Nat Chem Biol*, 2017, 13, 226-234.
15. Y. Itoh, R. Johnson and B. Scott, *Current Genetics*, 1994, 25, 508-513.
16. S. Saikia, E. J. Parker, A. Koulman and B. Scott, *FEBS Letters*, 2006, 580, 1625-1630.
17. 5399582, 1995.
18. F. Namiki, M. Matsunaga, M. Okuda, I. Inoue, K. Nishi, Y. Fujita and T. Tsuge, *Molecular Plant-Microbe Interactions*, 2001, 14, 580-584.
19. C. Liu, A. Minami, M. Noike, H. Toshima, H. Oikawa and T. Dairi, *Appl. Environ. Microbiol.*, 2013, 79, 7298-7304.